

RSC Advances



This is an *Accepted Manuscript*, which has been through the Royal Society of Chemistry peer review process and has been accepted for publication.

Accepted Manuscripts are published online shortly after acceptance, before technical editing, formatting and proof reading. Using this free service, authors can make their results available to the community, in citable form, before we publish the edited article. This *Accepted Manuscript* will be replaced by the edited, formatted and paginated article as soon as this is available.

You can find more information about *Accepted Manuscripts* in the [Information for Authors](#).

Please note that technical editing may introduce minor changes to the text and/or graphics, which may alter content. The journal's standard [Terms & Conditions](#) and the [Ethical guidelines](#) still apply. In no event shall the Royal Society of Chemistry be held responsible for any errors or omissions in this *Accepted Manuscript* or any consequences arising from the use of any information it contains.

1 **Core-shell polysiloxane-MOF 5 microspheres as stationary phase for gas-solid**
2 **chromatographic separations**

3
4 Manju^{a,b}, Prasun Kumar Roy^{a*}, Arunachalam Ramanan^{b*}, Chitra Rajagopal^a

5

6

7 ^aCentre for Fire, Explosive and Environment Safety, DRDO, Delhi-54, India

8 ^bDepartment of Chemistry, Indian Institute of Technology Delhi, New Delhi-16, India

9

10

11

12

13

14

15

16

17

18

19

20 *Corresponding Authors

21 Arunachalam Ramanan: aramanan@chemistry.iitd.ac.in

22 Prasun Kumar Roy: pk_roy2000@yahoo.com

1
2
3
4
5
6
7
8

Abstract

Core-shell poly(dimethylsiloxane) (PDMS)-MOF 5 microspheres were prepared by directed crystallization of MOF 5 on thermally stable PDMS beads. The microspheres were evaluated for their potential use as stationary phase for gas-chromatographic separation of permanent gases and liquids, where the issues associated with pressure drop were circumvented. The successful demonstration of this simple and versatile methodology widens the scope for large-scale application of Metal Organic Frameworks (MOFs) towards chromatographic separation.

1. Introduction

In view of their intriguing structures, exceptionally high surface areas, selective adsorption and high thermal stability, metal organic frameworks (MOFs) present immense potential in various fields, particularly for gas storage and separation.¹⁻⁴ The crystalline network formed by the self assembly of metal ions and multidentate organic linkers present ample scope in terms of in-pore functionalization and outer-surface modification to enable favourable interactions based on both “molecular sieving” as well as “chemical affinity” rendering these materials ideal for gas/liquid mixture separation. Lately numerous studies illustrating the potential of MOFs towards gas chromatographic separations have been reported,⁵ but have not been exploited at an industrial level.

Efficient chromatographic separation in packed columns require the particle size of stationary phase to be large enough to circumvent issues associated with pressure drops (See Supplementary section). The pressure drop in a packed column is inversely proportional to the particle size, and it becomes increasingly impractical to drive the carrier gas in columns containing smaller particles. Early studies on MOF based chromatographic separations on packed beds relied on large crystals⁶⁻⁸ or MOF pellets⁹ in relatively short column (2-5 cm). To evade the pressure drop issue, researchers have lately directed their attention towards MOF coated capillary columns which additionally result in efficient separations.^{4, 10, 11} However, these columns are rather fragile, and suffer from their inherent problems, arising from uncontrolled film formation on the inner capillary walls. Also, capillary columns require relatively specialized injectors and ancillary flow and pressure controllers. Unfortunately, large scale synthesis of MOFs can only afford polycrystalline materials, which cannot be directly packed in chromatographic columns for reasons mentioned above. To envisage economically

1 viable chromatographic applications of functional MOFs at an industrial level, it is desirable to
2 develop methodologies or processes for integrating smaller crystallites that are amenable for
3 scale-up.

4 We hypothesise that efficient MOF based separations can very well be performed on
5 conventional packed beds by immobilizing the MOFs on an inert template so as to increase the
6 particle size suitably for use in chromatographic columns. The core material has been selected
7 from the broad group of siloxanes, in view of their excellent thermal stability and their
8 widespread use as a template in the field of soft lithography,¹² and MOF 5 was selected based on
9 its celebrated nature. The crystal structure of $Zn_4(O)(BDC)_3$ or MOF 5 framework is made of
10 oxocentered Zn_4O connected through linear benzenedicarboxylate (BDC) units forming an
11 extended 3D cubic network with interconnected pores of 8 Å aperture width and 12 Å pore
12 diameter (Fig. 1). Inset shows oxo-centered Zn_4O tetrahedra connected through linear BDC
13 linkers creating open pores.

14 **Fig. 1:** Secondary building unit and crystal structure of MOF 5 (Zn: blue; C: grey; H: white and
15 O: red).

16 In this paper, we report a simple procedure for directed crystallisation of MOF 5 on the PDMS
17 microspheres, which have been subsequently employed as a stationary phase for gas
18 chromatographic separations. This route yields particles with core-shell morphology requiring
19 substantially lesser amount of MOFs, which is expected to result in lesser band broadening in the
20 chromatograms compared to fully porous materials, thereby delivering higher efficiencies. The
21 methodology can be applied to prepare any PDMS (core)-MOF (shell) combination, and can be
22 used to generate novel stationary phase for chromatographic separations.

1 **2. Materials and methods**

2 **2.1. Starting materials**

3 Silicone resin (Elastosil M4644) and the platinum based hardener was obtained from Wacker,
4 Germany. PVA (Mol. wt. 14000, CDH), Zinc nitrate trihydrate ('AR' grade, E.Merck),
5 terephthalic acid (TPA) ('AR' grade, E. Merck), N,N- Dimethylformamide (DMF) ('AR' grade,
6 E. Merck) and chloroform (CDH) were used without any further purification. Distilled water was
7 used throughout the course of study.

8 **2.2. Preparation of Core shell PDMS-MOF-5 microspheres**

9 The suspension curing of vinyl terminated methyl hydrosiloxane dimethylsiloxane at 45 °C in
10 the presence of a hydrosilylation catalyst was performed as per the procedure reported earlier.^{13,}
11 ¹⁴ The PDMS core was employed as a seed for directed crystallization of MOF 5 as per the
12 procedure reported previously.¹⁵ In brief, separate solution of terephthalic acid (TPA. 5.06 g,
13 30.5 mmol) and zinc acetate dihydrate (16.99 g, 77.4 mmol) were introduced into a suspension
14 of PDMS (10 g) in DMF, and allowed to react for ~2.5 h under stirring at 600 rpm, which
15 resulted in microspheres with core-shell morphology.

16

17 **2.3. Characterization**

18 The identification of crystalline phases in the sample was performed by powder X-ray diffraction
19 (PXRD) analysis on Bruker D8 advanced diffractometer using Nickel filter Cu-K_α radiation. The
20 data was collected with a step size of 0.02° and at count time of 1 sec per step over the range of
21 2°- 60° (2θ value). The effect of MOF-5 loading on the microsphere dimensions was determined
22 by a particle size analyser (DIPA 2000, Donner). Fourier Transform Infra-Red(FTIR) spectra of

1 samples were recorded in the wavelength range $4000 - 600 \text{ cm}^{-1}$ using a Thermo Fisher FTIR
2 (NICOLET 8700) analyser with an attenuated total reflectance (ATR) crystal accessory. The
3 textural properties of microspheres were determined by N_2 adsorption-desorption on a Surface
4 Area Analyzer (Micromeritics ASAP 2020). For this purpose, the sample was initially out gassed
5 under vacuum (10^{-6} Torr) at $200 \text{ }^\circ\text{C}$ for 16 h and the nitrogen adsorbate was pulsed at 77 K.
6 Surface area was calculated from the linear part of the Brunauer-Emmett-Teller(BET) plot and
7 Barrett–Joyner–Halenda (BJH) method was applied on the nitrogen desorption data to determine
8 the pore size distribution. Thermal degradation behaviour was investigated using Perkin Elmer
9 Diamond STG-DTA-DSC under N_2 atmosphere in the temperature range of $50\text{-}800 \text{ }^\circ\text{C}$. A
10 heating rate of $10 \text{ }^\circ\text{C}/\text{min}$ and a sample mass of $5.0 \pm 0.5 \text{ mg}$ were used for each experiment. The
11 surface morphology of samples was studied using a Scanning Electron Microscope(SEM) (Zeiss
12 EVO MA15) under an acceleration voltage of 20 kV. Samples were mounted on aluminium
13 stubs and coated with gold and palladium (10 nm) using a sputter coater (Quorum-SC7620)
14 operating at 10-12 mA for 120 s. The core shell structure was confirmed using Energy
15 Dispersion Analyser (EDS).

16

17 **2.4. Evaluation of core-shell microspheres for gas separation.**

18 The MOF 5 loaded PDMS microspheres were sieved to obtain particles of 60-80 mesh BSS
19 ($177\text{-}250 \text{ }\mu\text{m}$), which were packed in a stainless steel column (2 m length x 0.025 m diameter)
20 for evaluation of its efficiency towards separation of gaseous and liquid mixtures. A gas
21 chromatograph (NUCON, India), equipped with Thermal Conductivity Detector (TCD) and
22 Flame Ionization Detector (FID) was used for detection of the gaseous eluents. The prepared
23 column was pre-activated under a continuous flow of argon at $200 \text{ }^\circ\text{C}$ for 24 h. Standard mixture

1 of gases and liquids were injected into the column and the response of TCD and FID was
2 recorded to generate the gas chromatogram.

3

4 **3. Results and Discussion**

5 In this paper, we report a simple procedure for preparation of core shell poly(dimethylsiloxane)–
6 MOF 5 microspheres, which have been subsequently employed as a stationary phase for gas
7 chromatographic separations.

8

9 **3.1. Suspension curing of siloxane**

10 Suspension polymerisation of vinyl terminated methyl hydrosiloxane dimethylsiloxane, in the
11 presence of a hydrosilylation catalyst led to the formation of smooth PDMS beads.¹³ The effect
12 of operating parameters on the particle dimensions is presented in **Fig. S1 (Supplementary**
13 **Information)**, which reveal that the particle size distribution shifts towards larger sized
14 microspheres with increasing polymerisable content in the dispersed oily droplets. In all cases,
15 complete conversion (> 98%) was achievable, as evidenced by gravimetric analysis.

16

17 **3.2. Effect of MOF-5 loading on the microsphere dimensions and morphology**

18 The surface morphology of PDMS core and core-shell microspheres as revealed by Scanning
19 Electron Microscopy (SEM) are presented in **Fig. 2 a, b**. Magnified image of MOF 5 crystallites
20 on the surface are also presented in the inset of Fig. 2 b. The presence of MOF 5 on the surface

1 of core-shell microspheres was further confirmed by EDS analysis, which indicate the presence
2 of zinc in the shell region of the microsphere.

3 **Fig. 2:** Surface morphology and elemental analysis of (a) PDMS and (b) Core-shell PDMS-MOF
4 5 microspheres. Inset shows the magnified image of MOF 5 crystallites on the surface

5 The BET surface area was determined by physisorption of N₂ at 77 K. The adsorption-desorption
6 isotherms of the MOF 5 loaded microspheres and the core PDMS are presented in Fig. 3. PDMS
7 microspheres exhibited non-porous nature as evidenced by negligible nitrogen uptake and low
8 surface area (8 m²/g). The loading of MOF 5 on the core PDMS resulted in a tremendous
9 increase in the surface area (2850 m²/g) and the corresponding adsorption isotherms revealed its
10 characteristic microporous nature. To evaluate the adherence of the MOF 5 coating onto the core
11 PDMS, the MOF 5 loaded microspheres were soaked in DMF for 30 min, followed by exposure
12 to ultrasonic water bath (operating frequency 33 KHz) for 15 min. The coating adhered strongly,
13 with the extent of mass loss being negligible (<2%), as estimated gravimetrically.

14
15 **Fig. 3:** N₂ adsorption (open symbol) and desorption isotherms (filled symbol) for PDMS-MOF 5.
16 Inset shows the adsorption-desorption isotherms of core PDMS

17 The PXRD pattern of the siloxane core and PDMS-MOF 5 is presented in Fig. 4, which clearly
18 reveals the amorphous nature of PDMS. On the other hand, the XRD of MOF 5 loaded PDMS
19 exhibit distinct diffraction peaks, and the peak positions match with the powder pattern generated
20 by Crystallographic Information File (CCDC-277428).

21 **Fig. 4:** PXRD of a) PDMS b) PDMS-MOF 5

1 The TGA traces of the siloxane core, MOF 5 and core shell microspheres (PDMS-MOF 5) are
2 presented in Fig. 5, which reveal that prepared microspheres exhibit excellent thermal stability
3 and can be used in service till 250 °C.

4 **Fig. 5:** TG traces of (a) MOF 5, (b) PDMS-MOF 5 and (c) PDMS

5 The FTIR of the PDMS, both before and after MOF loading is presented in Fig. 6. In the FTIR
6 spectra of PDMS, characteristic absorption at 802 and 1258 cm^{-1} were observed which could be
7 attributed to the $(\text{CH}_3)_2\text{SiO}$ group vibration in the polymer. Additionally a broad absorption at
8 1000-1130 cm^{-1} was also observed, which can be attributed to the Si-O-Si vibration. Due to the
9 coordination of the carboxylic acid groups with the metal ions, there is a significant shift in the
10 position of the CO absorption band, from 1676 cm^{-1} , in TPA, to 1657 cm^{-1} in MOF 5 (Fig. 6b).
11 Coordination of the linker with the metal ions leads to the disappearance of the CO absorption
12 band at 1281 cm^{-1} and the broad absorption due to the hydroxyl groups $\sim 3000\text{-}3200 \text{ cm}^{-1}$.

13 **Fig. 6:** FTIR spectra of (a) PDMS (b) PDMS-MOF 5 microspheres

14 3.3. Gas-chromatographic separations

15 A standard mixture (50 μL) of permanent gases in (59.03% H_2 , 20.05% N_2 , 5.05% CH_4 , 10.0%
16 CO_2 and 5% CO , (% v/v) (Sigma gases) was injected into the GC column and the chromatogram
17 in terms of the detector response is presented in Fig. 7.

18 **Fig. 7:** Gas chromatograms showing effective separations of H_2 , N_2 , CO , CH_4 and CO_2 . Inset
19 shows the gas chromatogram exhibiting excellent separation of liquids

20 The retention time of each component, as determined by injection of individual gas separately, is
21 given in the supplementary section (see Table. S1, ESI†). The order of elution of the individual

1 gases from the column is in accordance with increasing order of their kinetic diameters (H_2 , 2.89
2 Å; N_2 , 3.64 Å; CO , 3.76 Å; CH_4 , 3.8 Å and CO_2 , 3.3 Å). It is to be noted that the estimated pore
3 size of MOF 5 is too large ($\sim 9\text{Å}$) to permit separations based on molecular sieving, and hence the
4 sequence of elution is very well expected. Interestingly, CO_2 with a kinetic diameter of 3.3 Å
5 elutes at the end, which can be explained on the basis of strong interaction of CO_2 with the MOF
6 5 framework.¹⁶ The efficiency of the packed PDMS-MOF 5 column towards separation of
7 liquids was also established by injecting an equimolar mixture of methanol, propanol and
8 acetone which were detected using flame ionisation technique. The chromatogram (response of
9 FID) as shown in the inset of Fig. 7, clearly establishes the ability of the column towards
10 separation of liquid mixtures. Since the kinetic diameter of all the molecules is lesser than the
11 pore size of MOF-5, the order of elution is in line.

12 For comparison purpose, chromatographic separations were also performed on commercially
13 available packed columns generally employed for separation of similar gas mixtures, namely
14 molecular sieve 5A (MS 5) and Porapak N. The chromatograms obtained are shown in the
15 supplementary section, (see supplementary section, ESI†). Carbon dioxide does not elute from
16 MS 5 column due to its strong interactions with the microporous aluminosilicate structure, while
17 Porapak N is incapable of separating H_2 and N_2 mixture.¹⁷ It can be seen that neither of these
18 columns individually could separate all the components, however a 2D separation can be used
19 for effective separations.

20
21 The prepared column was also employed to separate a natural gas mixture comprising of 79.37%
22 Methane, 6.72% Ethane, 0.94% Iso-Butane, 0.53% Iso-Pentane, 1.31% N-Butane, 0.19% N-
23 Hexane, 0.51% N-Pentane, 8.09% Propane and 2.34% CO_2 (%v/v). For this purpose, 50 μL of

1 the gas mixture was injected into the GC column and the separation was effected under
2 conditions mentioned in the supplementary section. The TCD response is presented in Fig. 8.
3 The retention time of each component, as determined by injection of individual gas separately, is
4 given in the supplementary section (see Table. S2, ESI†). It can be seen that all the components
5 could be effectively separated by the PDMS-MOF 5 column.

6
7 **Fig. 8:** Gas chromatogram showing separation of natural gas mixture. 1. Methane, 2. Ethane, 3.
8 Propane, 4. Carbon dioxide, 5. Iso-Butane, 6. n-Butane, 7. n-Pentane, 8. n-Hexane.

9 Our study clearly highlights the potential of MOF loaded microspheres for practical application
10 towards separation of gas mixtures. The reproducibility of the PDMS-MOF 5 column was
11 established by performing repeated runs on gas mixtures obtained from ethanol reforming exit
12 stream,¹⁸ comprising primarily of H₂, N₂, CH₄, CO₂ and CO, which corroborates excellent
13 separation reproducibility.

14 It should be noted that in view of tunability of the pore size of MOFs by judicious choice
15 of SBU and linker molecules, it is possible to envisage hitherto unprecedented separations,
16 thereby opening novel opportunities in the field of separation technology.

17 **4. Conclusions**

18 We demonstrate the potential of core-shell PDMS-MOF 5 for effective separation of gas/liquid
19 mixtures in a packed chromatographic column, where the issues associated with pressure drop
20 are circumvented. It should be noted that the methodology reported here could in principle be

1 applied towards crystallisation of any MOF. The ease of this technique suggests scope for wider
2 applicability of MOFs in the field of chromatographic separations.

3 **Acknowledgement**

4 The authors are thankful to Dr Sudershan Kumar, Director, Centre for Fire, Explosive and
5 Environment Safety for taking keen interest and for providing the laboratory facilities. The
6 authors also gratefully acknowledge the help extended by Gyan Batra, NUCON, Delhi India, for
7 preparation of the packed SS columns for chromatographic separation.

9 **References**

- 10 1. H. Furukawa, N. Ko, Y. B. Go, N. Aratani, S. B. Choi, E. Choi, A. Ö. Yazaydin, R. Q.
11 Snurr, M. O’Keeffe, J. Kim and O. M. Yaghi, *Science*, 2010, **329**, 424-428.
- 12 2. S. L. James, *Chem. Soc. Rev.*, 2003, **32**, 276-288.
- 13 3. U. Mueller, M. Schubert, F. Teich, H. Puetter, K. Schierle-Arndt and J. Pastre, *J. Mater.*
14 *Chem.*, 2006, **16**, 626-636.
- 15 4. R. Ahmad, A. G. Wong-Foy and A. J. Matzger, *Langmuir*, 2009, **25**, 11977-11979.
- 16 5. C. Montoro, F. Linares, E. Q. Procopio, I. Senkovska, S. Kaskel, S. Galli, N. Masciocchi,
17 E. Barea and J. A. R. Navarro, *J Am Chem Soc*, 2011, **133**, 11888-11891.
- 18 6. B. Chen, C. Liang, J. Yang, D. S. Contreras, Y. L. Clancy, E. B. Lobkovsky, O. M. Yaghi
19 and S. Dai, *Angew. Chem. Int. Ed.*, 2006, **45**, 1390-1393.
- 20 7. S. Han, Y. Wei, C. Valente, I. Lagzi, J. J. Gassensmith, A. Coskun, J. F. Stoddart and B.
21 A. Grzybowski, *J. Am. Chem. Soc.*, 2010, **132**, 16358-16361.

- 1 8. T. Borjigin, F. Sun, J. Zhang, K. Cai, H. Ren and G. Zhu, *Chem. Commun.*, 2012, **48**,
2 7613-7615.
- 3 9. D. Peralta, G. Chaplais, J.-L. Paillaud, A. Simon-Masseron, K. Barthelet and G. D.
4 Pirngruber, *Microporous Mesoporous Mater.*, 2013, **173**, 1-5.
- 5 10. Z.-Y. Gu, D.-Q. Jiang, H.-F. Wang, X.-Y. Cui and X.-P. Yan, *J. Phys. Chem. C*,
6 2009, **114**, 311-316.
- 7 11. Z.-L. Fang, S.-R. Zheng, J.-B. Tan, S.-L. Cai, J. Fan, X. Yan and W.-G. Zhang, *J.*
8 *Chromatogr. A*, 2013, **1285**, 132-138.
- 9 12. L. Wang, W. Jiang, X. Chen, L. Gu, J. Chen and R. T. Chen, *J. Appl. Phys.*, 2007,
10 **101**, -.
- 11 13. P. K. Roy, M. Hakkarainen and A.-C. Albertsson, *Polym. Degrad. Stab.*, 2012, **97**,
12 1254-1260.
- 13 14. P. K. Roy, Manju, C. Rajagopal and A. Ramanan, *2766/DEL/2013*, 2013.
- 14 15. Manju, P. Kumar Roy, A. Ramanan and C. Rajagopal, *Mater. Lett.*, 2013, **106**, 390-
15 392.
- 16 16. Z.-Y. Gu and X.-P. Yan, *Angew. Chem. Int. Ed.*, 2010, **49**, 1477-1480.
- 17 17. J. W. Yoon, S. H. Jhung, Y. K. Hwang, S. M. Humphrey, P. T. Wood and J. S.
18 Chang, *Adv. Mater.*, 2007, **19**, 1830-1834.
- 19 18. P. K. Sharma, N. Saxena, A. Bhatt, C. Rajagopal and P. K. Roy, *Catal. Sci. Technol.*,
20 2013, **3**, 1017-1026.

21

List of Figures

Figure 1: Secondary building unit and crystal structure of MOF 5 (Zn: blue; C: grey; H: white and O: red).

Figure 2: Surface morphology and elemental analysis of (a) PDMS and (b) Core-shell PDMS-MOF 5 microspheres. Inset shows the magnified image of MOF 5 crystallites on the surface.

Figure 3: N₂ adsorption (open symbol) and desorption isotherms (filled symbol) for PDMS-MOF 5. Inset shows the adsorption-desorption isotherms of core PDMS.

Figure 4: PXRD of a) PDMS b) PDMS-MOF 5

Figure 5: TG traces of (a) MOF 5, (b) PDMS-MOF 5 and (c) PDMS

Figure 6: FTIR spectra of (a) PDMS (b) PDMS-MOF 5 microspheres

Figure 7: Gas chromatograms showing effective separations of H₂, N₂, CO, CH₄ and CO₂.

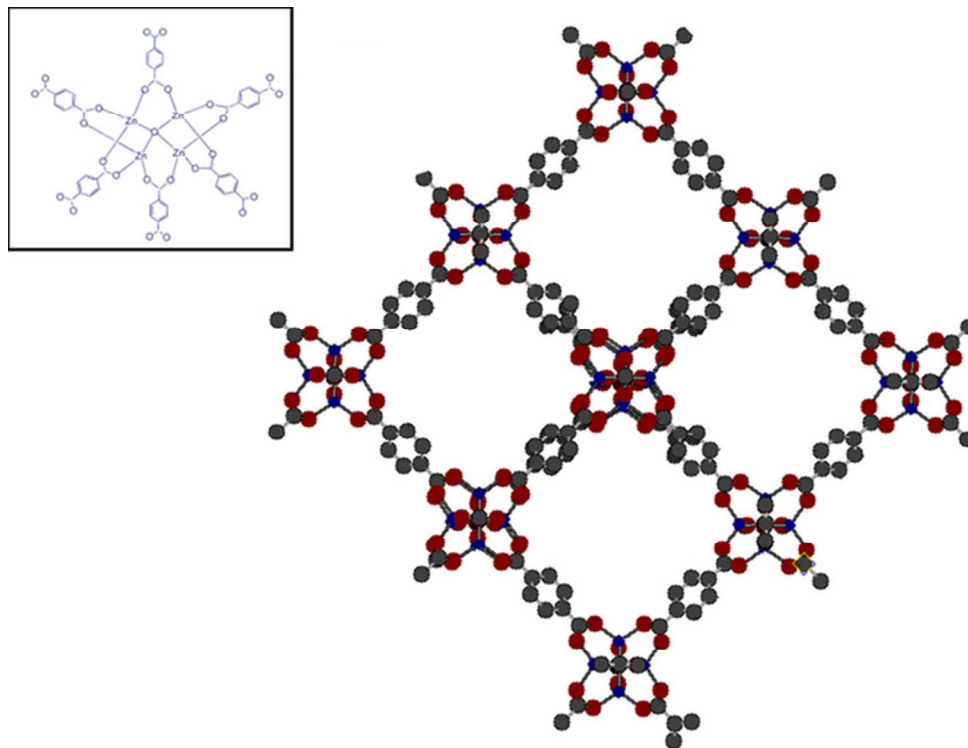
Inset shows the gas chromatogram exhibiting excellent separation of liquids

Figure 8: Gas chromatogram showing separation of natural gas mixture. 1. Methane, 2. Ethane, 3. Propane, 4. Carbon dioxide, 5. Iso-Butane, 6. n-Butane, 7. n-Pentane, 8. n-Hexane.

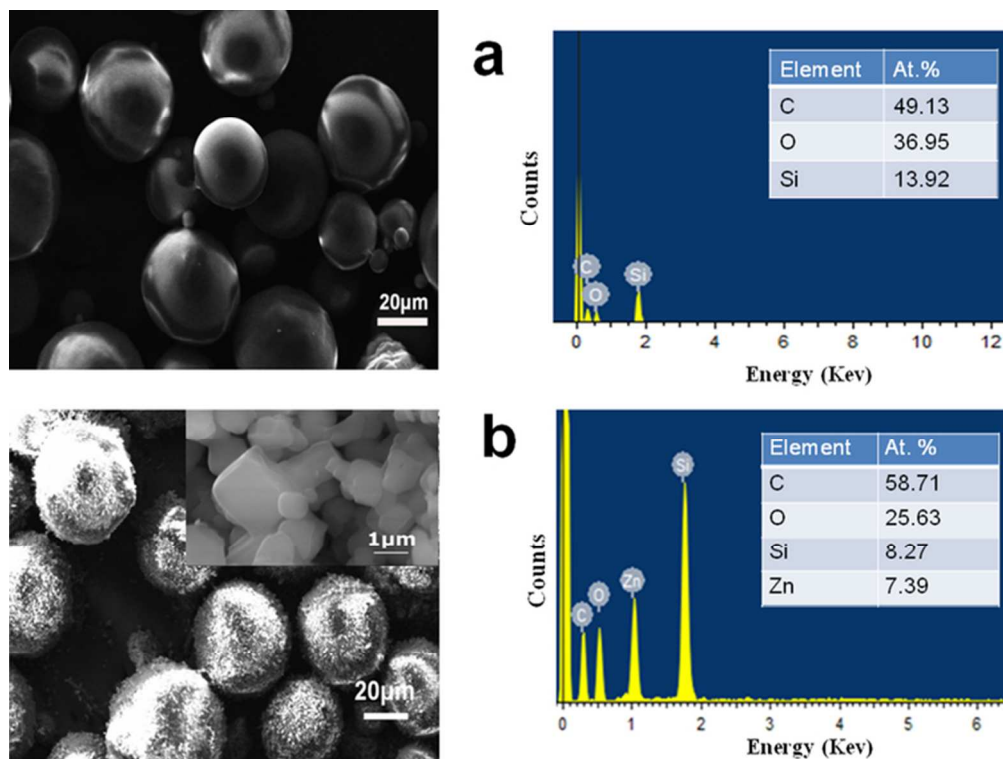
List of tables

Table S1: Retention time of the gaseous components present in the mixture (H₂, N₂, CH₄, CO₂ and CO) using core-shell PDMS -MOF 5 column

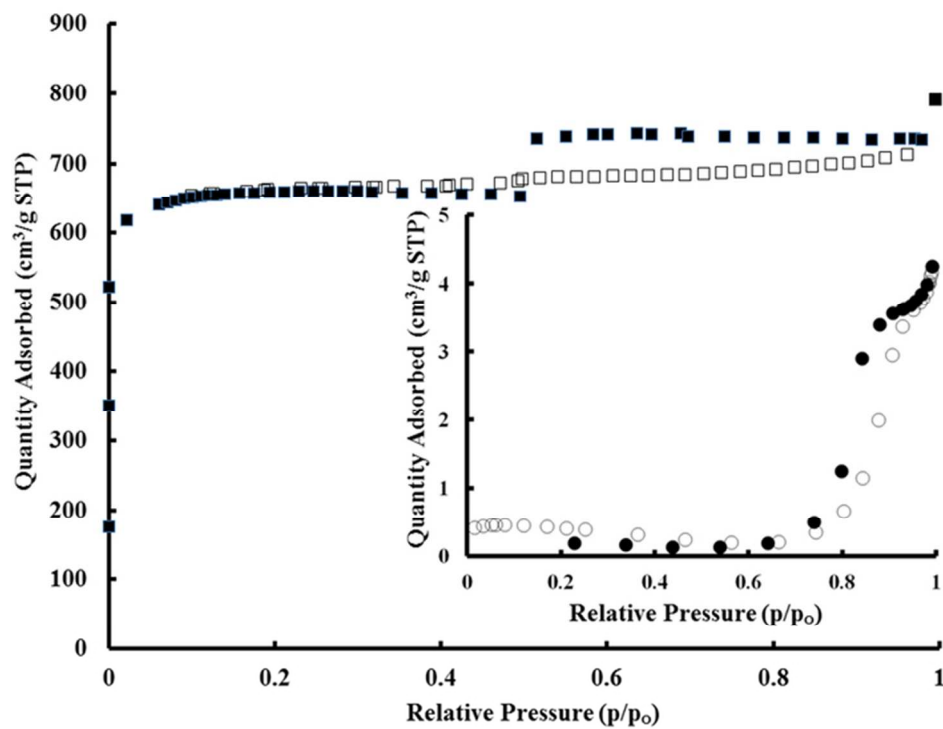
Table S2: Retention time of the gaseous components present in the natural gas mixture using core-shell PDMS -MOF 5 column.



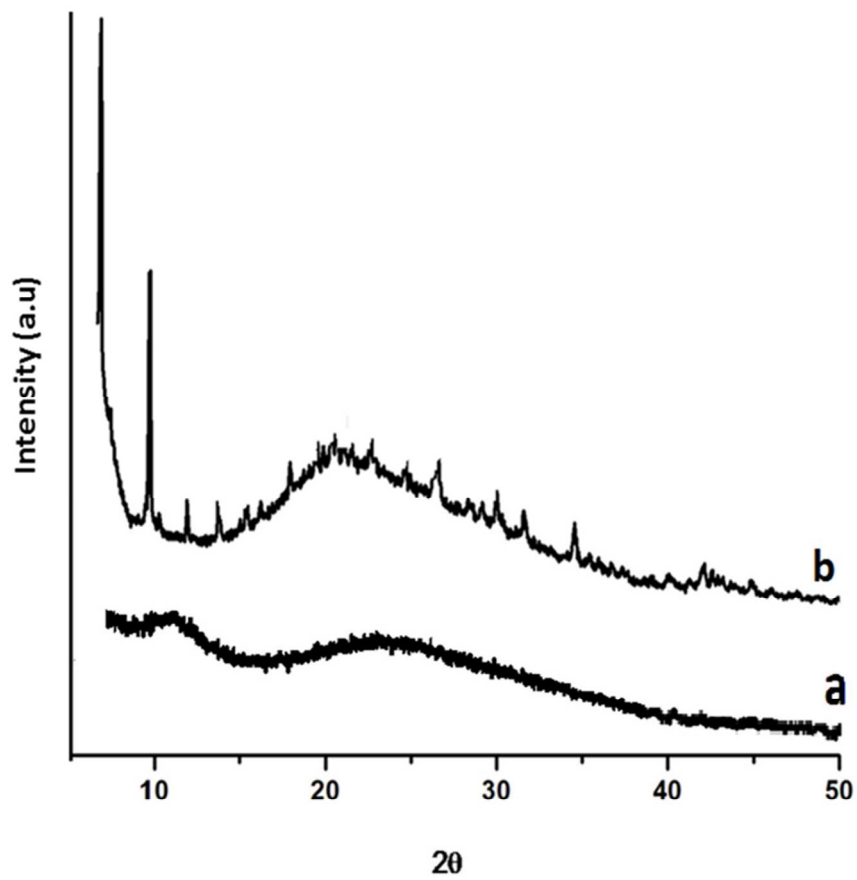
Secondary building unit and crystal structure of MOF 5 (Zn: blue; C: grey; H: white and O: red).
63x47mm (300 x 300 DPI)



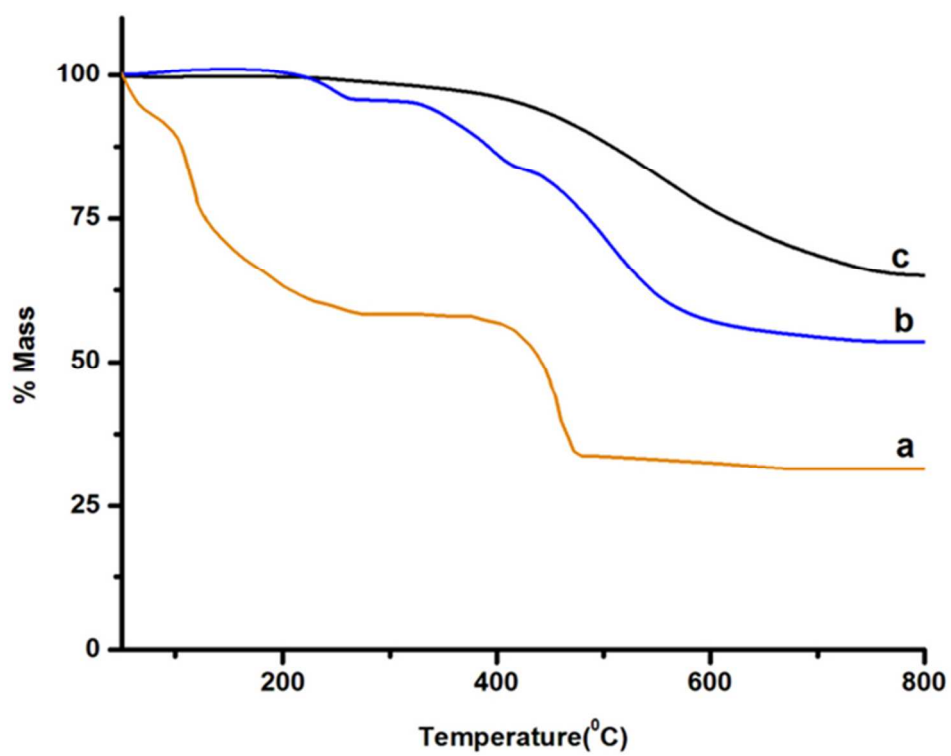
Surface morphology and elemental analysis of (a) PDMS and (b) Core-shell PDMS-MOF 5 microspheres. Inset shows the magnified image of MOF 5 crystallites on the surface. 63x47mm (300 x 300 DPI)



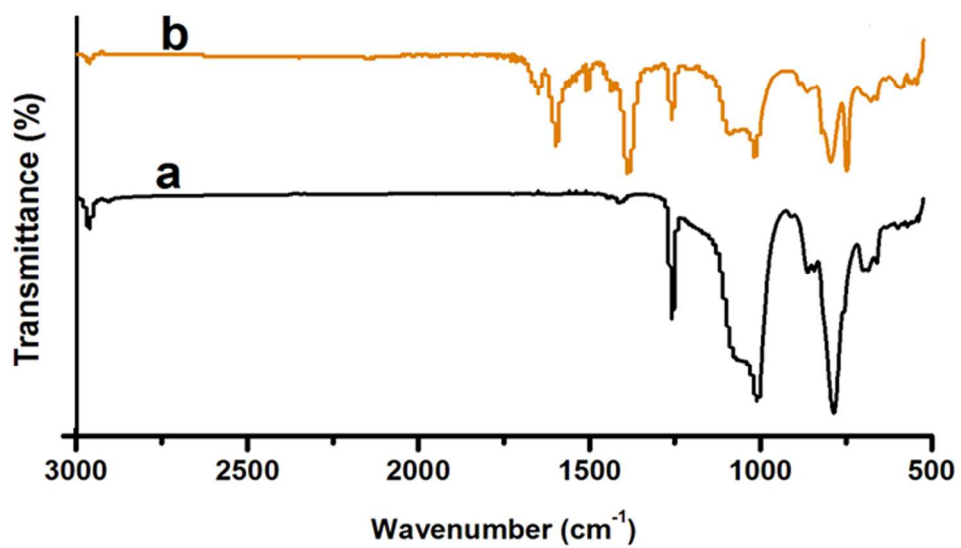
N₂ adsorption (open symbol) and desorption isotherms (filled symbol) for PDMS-MOF 5. Inset shows the adsorption-desorption isotherms of core PDMS.
63x47mm (300 x 300 DPI)



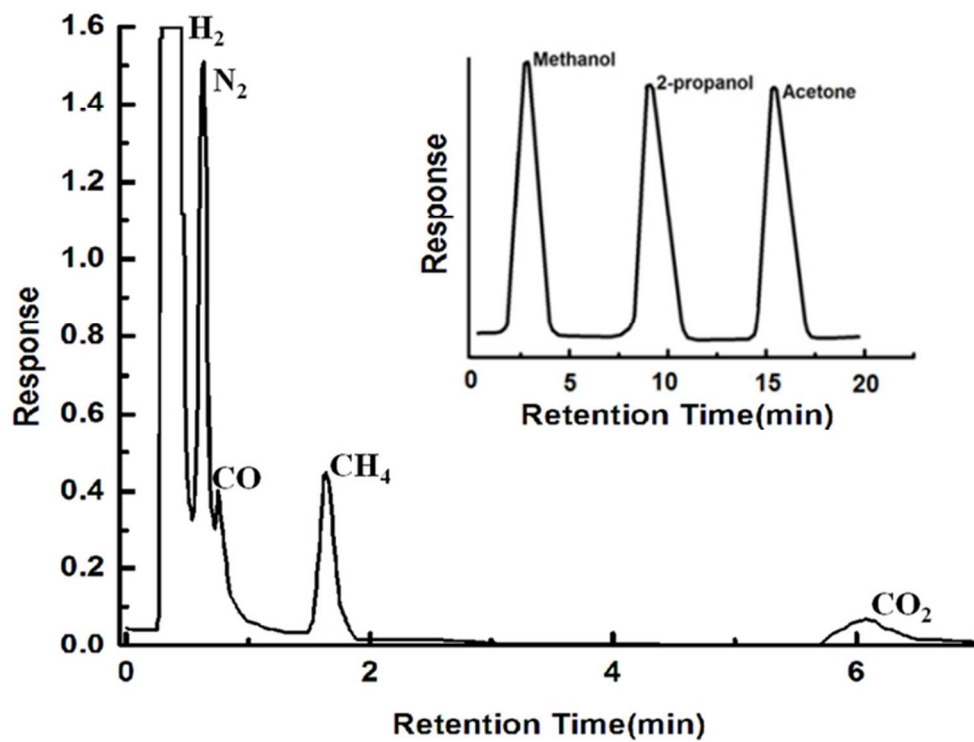
PXRD of a) PDMS b) PDMS-MOF 5
76x69mm (300 x 300 DPI)



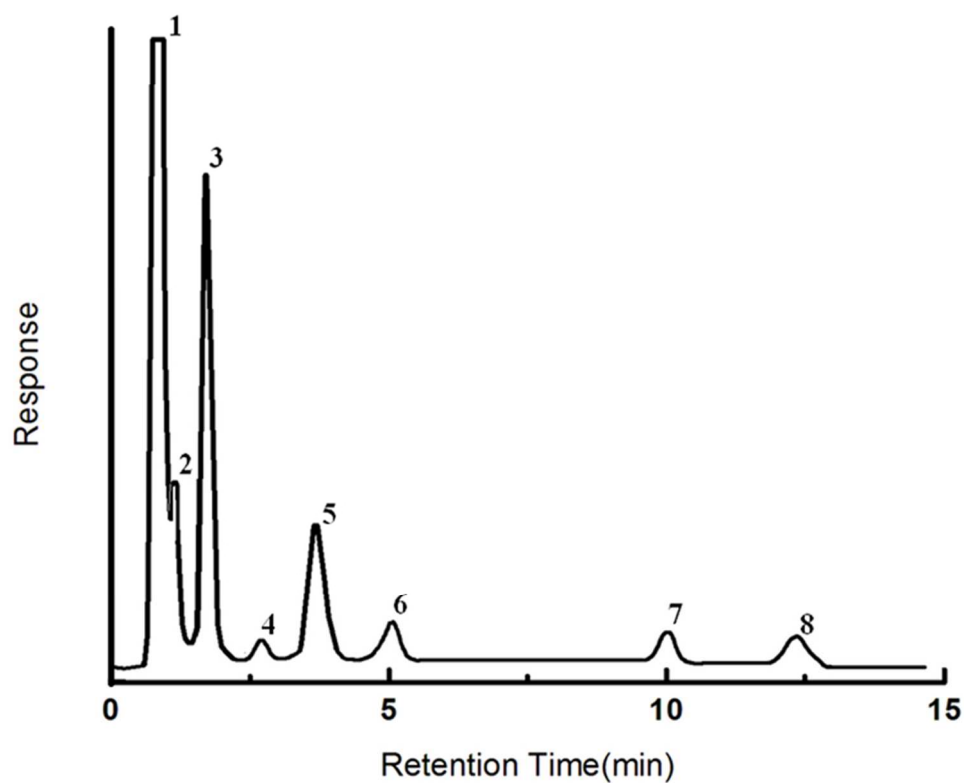
TG traces of (a) MOF 5, (b) PDMS-MOF 5 and (c) PDMS
67x53mm (300 x 300 DPI)



FTIR spectra of (a) PDMS (b) PDMS-MOF 5 microspheres
85x47mm (300 x 300 DPI)



Gas chromatograms showing effective separations of H₂, N₂, CO, CH₄ and CO₂. Inset shows the gas chromatogram exhibiting excellent separation of liquids
63x47mm (300 x 300 DPI)



Gas chromatogram showing separation of natural gas mixture. 1. Methane, 2. Ethane, 3. Propane, 4. Carbon dioxide, 5. Iso-Butane, 6. n-Butane, 7. n-Pentane, 8. n-Hexane.
69x56mm (300 x 300 DPI)